

Welding Residual Stresses in Two Competing Single V-Butt Joints

Pornwasa WONGPANYA

*School of Metallurgical Engineering, Suranaree University of Technology
Nakhon Ratchasima, 30000 Thailand*

Received Apr. 27, 2009

Accepted May 14, 2009

Abstract

During fabrication of welded components residual stresses are generated as a result of non-uniform temperature distribution during the welding and particularly the cooling processes. The residual stresses have a major effect on the overall performance of the components in service, especially when hydrogen is involved and the components might become prone to Hydrogen Assisted Cold Cracking (HACC). Up to the present, most of the welding standards and specifications to test the resistance of welds against HACC test are without consideration of the restraint intensity provided by the surrounding structure. This may lead to a misunderstanding of the welding heat treatment procedures, i.e. preheating and interpass temperature, for multi-pass welding of extra high strength steels. The restrained welds might also interact at real components with respect to the stresses and strains produced in the transverse direction. This point has not been addressed within recent years, and in order to elucidate such effects, two competing single v-butt joints in high strength steel with a yield strength level of 1100 MPa are investigated in the present contribution by Finite Element Analyses (FEA). As a specific result, it turned out that the transverse residual stresses increase with the restraint intensity of the surrounding structure. As a consequence of the different restraint intensity during completion of the joints, the stresses are distributed inhomogeneously in the component and special attention has to be paid to such regions with respect to cold cracking.

Key words : Residual stress, High strength steel, Restrain effect

Introduction

Over the past decades, High Strength Structural Steels (HSSS) have been used in many welded steel constructions. The reduction of weight is the most important advantage in using steels with yield strength levels of up to 1100 MPa in various industrial applications, i.e. for mobile cranes, bridge structures and pipelines. However, applications of such steels have been accompanied by failure cases that occur mostly as Hydrogen Assisted Cold Cracking (HACC) during fabrication and service.

A unique characteristic of HACC in welded components is generally promoted by three main interrelated factors, i.e. susceptible microstructure, hydrogen concentration and residual stress, as shown in Figure 1. In order to solve such failure cases, many techniques are used in control of HACC in the weld based on the reduction of hydrogen input, pre- and postheating and heat input consideration. Certain techniques can be used to remove some

critical factors, i.e. hydrogen concentration and susceptible microstructure, but the interaction of the thermal cycle with the components reaction in terms of stress build up has not been completely understood, particularly with respect to HACC avoidance.⁽¹⁾ Therefore, this paper will discuss predominantly the topic of welding residual stresses in the single V-butt joints of three plates.

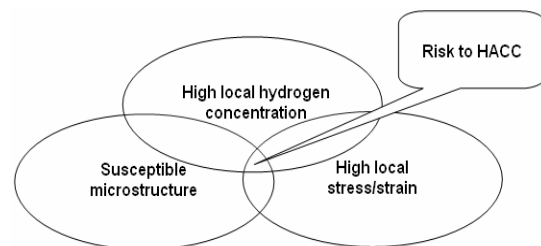


Figure 1. Three main interrelated factors encourage HACC in welded structures

Traditionally, welding residual stresses are produced by three main processes⁽²⁾:

1. Residual stresses due to shrinkage process
2. Residual stresses due to quenching process
3. Residual stresses due to phase transformation

It was found that the external load or stiffness of the surrounding construction significantly increases both the transverse and longitudinal welding residual stress, as shown in Figure 2. As a further point, in real welded components the interaction between the stresses resulting from welding with further (external) service loads still has to be clarified, with respect to avoidance of delayed cold cracking within the initial periods of service operation.⁽³⁻⁵⁾

The structural stiffness in the vicinity of a joint is providing a shrinkage restraint that significantly influences the thermal-mechanical loads introduced during welding and, in particular, cooling of a specific joint in any component. For better understanding the structural effect, the principle of considering the stiffness by the total restraint intensity produced in the weld has to be understood first of all.

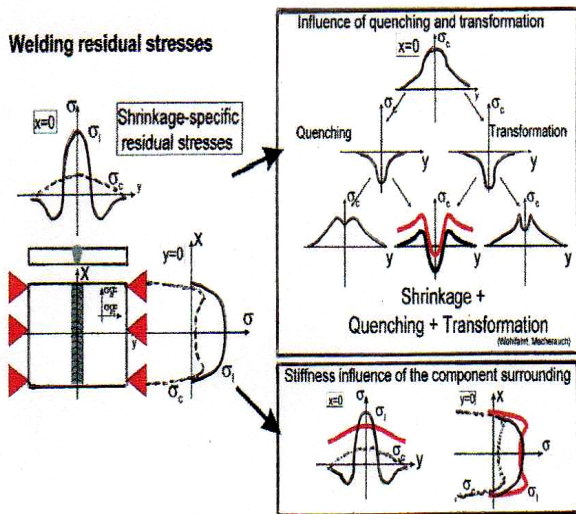


Figure 2. Schematic illustration of four main factors producing welding residual stress

The basic concept of restraint intensity has been introduced by Satoh, *et al.* 1973. in the early 1970s and allows consistent evaluation of the shrinkage restraint transverse to the weld. Consider a specific amount of free shrinkage S_y as shown in Figure 3 transverse to the weld which is caused by thermal contraction during cooling process of the weld.

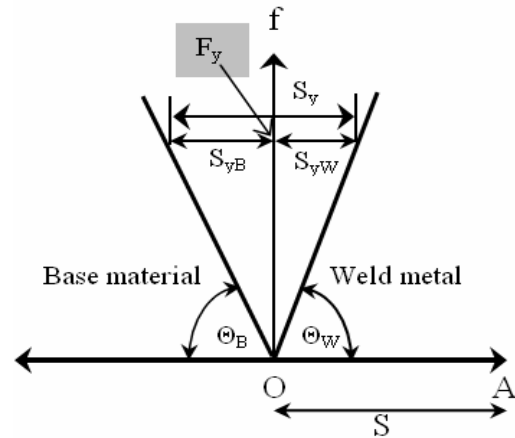


Figure 3. Schematic illustration of shrinkage restraint condition of the base material producing different reaction forces and deformations in the base material and the weld metal⁽⁶⁾

When two bars are connected by welding with high external forces, the movement of the bars is not possible and thus, a reaction force F_y is introduced which has to be taken up by the base material and the weld metal, leading to respective displacements in the base material and the weld metal, S_{yB} and S_{yW} , respectively. Finally the total amounts of displacements in the weld are

$$S_y = S_{yB} + S_{yW} \tag{1}$$

Under this consideration, the shrinkage restraint R_s provided by the base material can be described by the tangent of the angle Θ_B , represented by the reaction forces produced in the weld metal divided by the respective base material displacement. The shrinkage restraint can thus be taken as a spring constant which the base material represents for the specific weld.

$$R_{yB} = \tan \Theta_B = \frac{F_{yB}}{S_{yB}} \tag{2}$$

In order to achieve a common unit for the shrinkage restraint the reaction forces have been unified by the weld metal length l_w . Such unified reaction forces produce a unit root gap displacement Δy ($\approx S_{yB}$) on the welds, which leads to the definition of restraint intensity R_{Fy} (Figure 4). It can thus be evaluated by the transverse reaction forces F_y related to the respective root gap displacement in both transverse directions $2 \cdot \Delta y$, normalized by the total weld length l_w :

$$R_{F_y} = \frac{F_y}{2\Delta y \cdot l_w} \quad (3)$$

Satoh, *et al.*⁽⁶⁻⁷⁾ also proposed a direct relation between the transverse reaction stresses σ_y and the restraint intensity as following

$$\sigma_y = p_o \cdot R_{F_y} \quad (4)$$

where p_o is proportional factor including the physical material properties and the welding parameters.

$$p_o = \frac{S_y}{h_w} = \alpha_T \cdot \sqrt{\frac{T_s \cdot q_m \cdot \tan \alpha}{c}} \quad (5)$$

where h_w , α_T , T_s , q_m , α and c are the weld metal height, thermal expansion coefficient, melting temperature of the weld metal, heat quantity, apex angle of the weld and specific heat capacity, respectively.

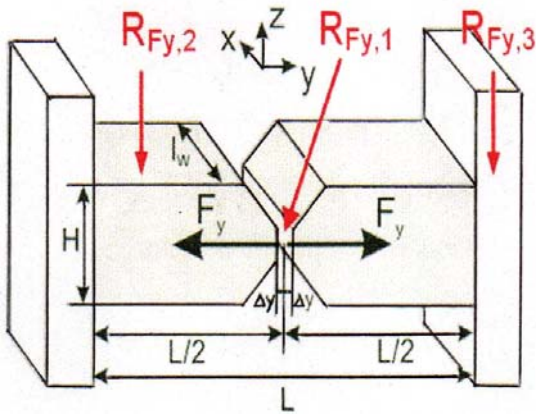


Figure 4. Schematic illustration relating to the definition of the restraint intensity $R_{F_y, total}$ for symmetric joint⁽³⁾

In general, the total restraint intensity produced in the weld is dependent on the three main factors, i.e. edge preparation ($R_{F_y,1}$), the plate dimensions ($R_{F_y,2}$) and the surrounding construction or external force ($R_{F_y,3}$). These three main factors contribute individually to the intensity of restraint and thus, these three parts have to be evaluated to calculate the total restraint intensity ($R_{F_y, total}$) of a weld by

$$\frac{1}{R_{F_y, total}} = \frac{1}{R_{F_y,1}} + \frac{1}{R_{F_y,2}} + \frac{1}{R_{F_y,3}} \quad (6)$$

However, the above consideration has been undertaken so far only at one joint for two plates, mostly butt and fillet welds. But, in the present case of two competing welds, the principle has to be transferred to a three plate joint, as illustrated in Figure 5.

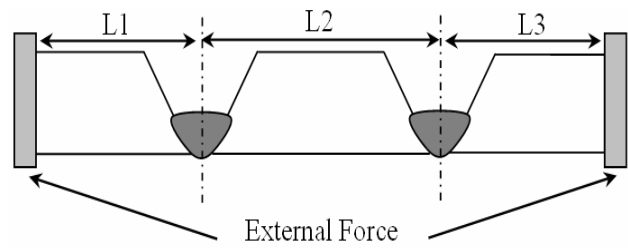


Figure 5. Three plates with single V-butt joints and application of external force

Materials and Experimental Procedures

Background

As this is a continuing approach of the previous investigation at a single V-butt joint (Figure 6a), the same shape has been applied to the two competing welds for comparison. (Figure 6b)^(1, 8-9) The previous results already showed that obtained temperature histories at the surface of the IRC test plates at a distance of 25 mm from the centreline of the weld bead are fairly consistent. The IRC test was first developed by Hoffmeister⁽⁸⁾ in order to measure the reaction forces and moments during welding and subsequent cooling. The test has been extensively applied to avoid cold cracking of the experimentally and numerically linear welds, and to investigate the effects of heat input as well as pre- and postheating on the reaction force, and stress build up during cooling after welding of specifically restrained joints. These are the reasons why the IRC test is selected to evaluate cold cracking risk.

Moreover, the strain level obtained from Finite Element Modelling (FEM) showed a good agreement with the experiment measuring by using rosette strain gauge located at the bottom and at the distance of 20 mm from the weld centreline. This means that stress distribution build up during welding and subsequent cooling can be evaluated successfully

by FEM. As a consequence, the procedure for the single weld can reliably be transferred to the two welds.

Materials

S 1100 QL steel is considered for evaluation in this study because this type of steel represents the maximum yield strength level of the modern high strength steels in the present period of time. The other reason for selecting this material is due to the fact that there is no existing standardization for cold cracking avoidance and welding procedure in welding of such material. This means that it is still a challenging task to find the proper welding procedure for this material in particular cold cracking avoidance. The chemical compositions of the base material and filler material are shown in Table 1.

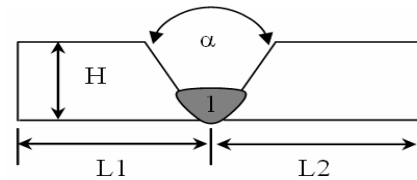
Table 1. Chemical compositions of S 1100 QL and Union X96

Material	C	Si	Mn	Cr	Mo	Ni
S 1100 QL	0.17	0.27	0.85	0.46	0.45	1.88
Union X96	0.12	0.78	1.86	0.46	0.53	2.36

Geometry of Joints

As described previously in the introduction, the restraint intensity of a welded joint is one of the means of evaluating the magnitude of the residual stresses and the susceptibility to weld cracking for mechanical reasons. Furthermore, in order to clarify the effects of plate dimension and the stress interaction between them on the restraint intensity and subsequent the residual stress distribution, three plates are being welded with various restraint lengths between them (L_2 , Figure 6b), i.e. the restraint length of $L = 55$ mm and $L = 110$ mm. In order to perform the worst-case assessment, rigidly clamping forces have been applied at the end of the model. Finally, the thermal-mechanical results of welding three plates have to be compared with that of welding two plates.

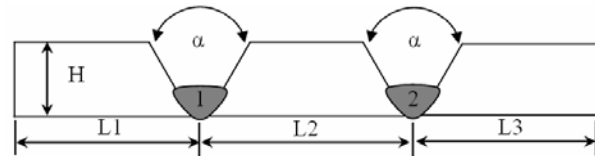
The overview of the different dimensions of the single V-butt joints for two and three plates, which have to be modeled, are summarized in Figure 6.



$$H = 20 \text{ mm}$$

$$L_1 = L_2 = 55 \text{ mm}, \alpha = 60^\circ$$

(a) Plate dimension for two-welded plates



Case I:

$$H = 20 \text{ mm}$$

$$L_1 = L_2 = L_3 = 55 \text{ mm}$$

$$\alpha = 60^\circ$$

Case II:

$$H = 20 \text{ mm}$$

$$L_1 = L_3 = 55 \text{ mm}$$

$$L_2 = 110 \text{ mm}$$

$$\alpha = 60^\circ$$

(b) Plate dimension and welding sequence for three-welded plates

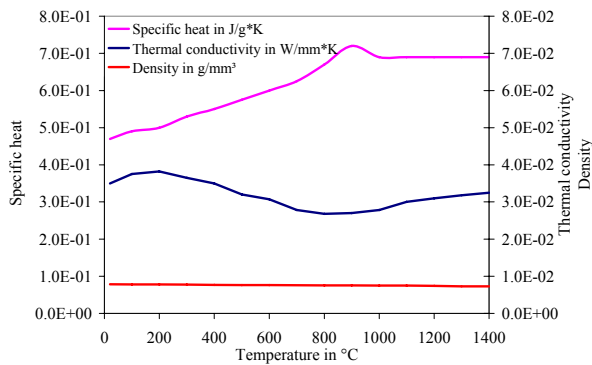
Figure 6. Overview of model dimension and welding Sequence

Numerical Approach

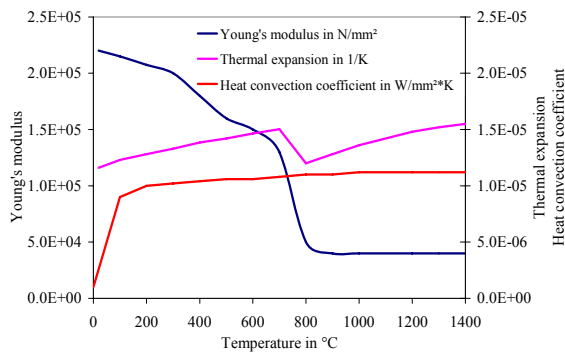
Material Properties

Most of the welding processes are based on a local heating of manufacturing parts up to melting temperature and then cooling them down. The temperature distribution is highly non-uniform both in spatial co-ordinates and in time. This non-uniform heating is a reason for residual stress in a welded component. It can be seen that the stress solution depends significantly on a temperature field. In addition, another important factor is that the temperatures calculated from thermal analysis are used as body forces for the subsequent thermo-mechanical analyses. The thermo-physical material properties such as density, heat convection coefficient, enthalpy and thermal conductivity will significantly affect the finally calculated stresses and strains. They have thus been selected very carefully from Richter's diagrams⁽¹⁰⁾ for steel with similar composition as the relatively new S 1100 QL type and have been applied to all microstructures of the joint, i.e. the weld metal, the Heat Affected Zone (HAZ) and the base material, as shown in Figure 7. Generally, the thermo-mechanical properties vary significantly with the weld microstructure. For instance, the yield strength and the ultimate tensile strength change drastically if the steel is austenitized during heating or if the austenite decomposes into a

martensitic-bainitic microstructure during cooling. Moreover, the percentage of martensite produced between the martensite start and finish temperature range follows a complex function. In this context, the true stress-strain behaviour was determined experimentally for the various simulated weld microstructures⁽¹¹⁻¹²⁾ and is shown in Figure 8. For simplification, the complex microstructure transformation processes were modeled by respective interpolation between the various temperature-dependent stress-strain curves and by the temperature dependent thermal expansion coefficients.



(a) Specific heat, thermal conductivity and density



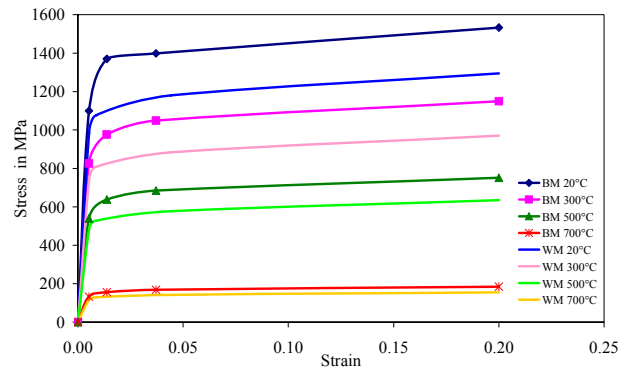
(b) Young's modulus, thermal expansion and heat convection coefficient

Figure 7. Temperature dependent thermo-physical properties for thermal analysis⁽¹⁰⁾

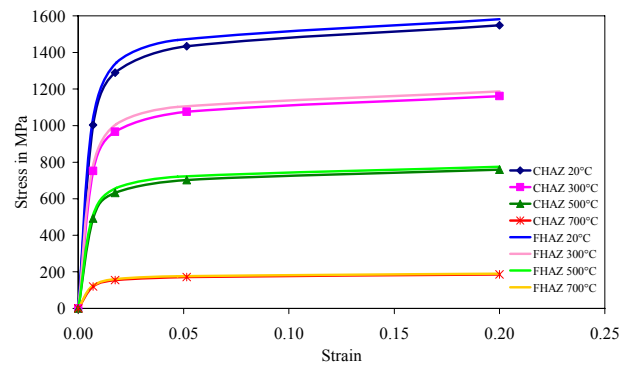
Calculation Procedure

In order to determine the residual stresses, indirectly coupled thermal and structural two dimensional analyses are carried out using the nodal results of the non-linear transient thermal calculations as body forces for the subsequent non-linear structural elastic-plastic numerical analysis, as represented in Figure 9. Thermal stresses can

then be calculated at each time increment, and the final state of accumulated residual stresses will be governed by the thermal strains and stresses.



(a) Modified values for base material (BM) and for weld metal (WM)



(b) Modified values for coarse and fine grain heat affected zone (CHAZ and FHAZ)

Figure 8. True stress-strain behaviour of S 1100 QL steel as thermo-mechanical properties for structural analysis

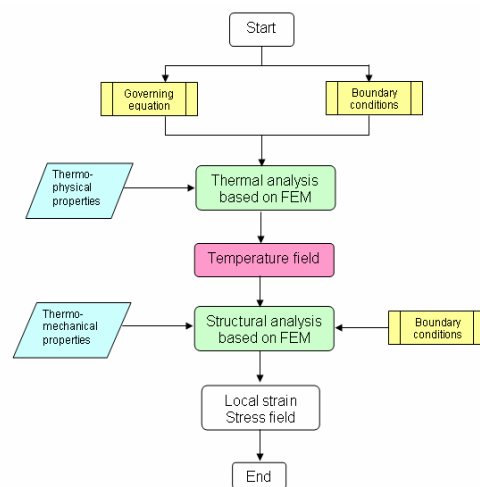


Figure 9. Flow chart of indirectly coupled thermal and structural two dimensional analyses

In order to simulate the heat dissipation into the clamping devices of the IRC Test or similarly, into a surrounding construction, a constant temperature has been assigned to both ends of the model. Heat convection has been modeled at all free surfaces of the joint. As described previously⁽¹³⁻¹⁴⁾, heat loss by radiation can be neglected for solid materials in contrast to liquids and has thus been ignored in the modeling procedure.

For the non-linear transient thermal-structural analysis, the boundary condition is that the plates being welded are rigidly clamped. To simulate such condition, both ends of the model are fixed in horizontal and vertical direction which is consistent with the rigid clamping in the respective IRC test.

Results and Discussion

Effect of Restraint Length on the Residual Stresses in Three-Welded Plates

Figure 10 and Figure 11 show transverse residual stress distribution in three-welded plates after cooling down to room temperature for rigidly clamping forces at both ends of the model with various restraint lengths, i.e. at $L_2 = 55$ mm and at $L_2 = 110$ mm, respectively.

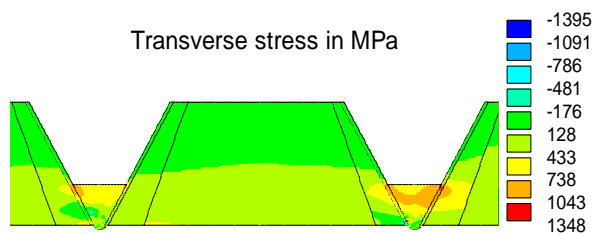


Figure 10. FEM calculated residual stresses distribution transverse to the welding direction in three-welded plates with restraint length of $L_2 = 55$ mm

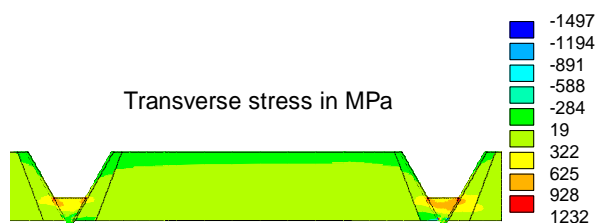


Figure 11. FEM calculated residual stresses distribution transverse to the welding direction in three-welded plates with restraint length of $L_2 = 110$ mm

Tensile stresses and compressive stresses are observed on the top surface and the bottom surface, respectively, indicating a bending effect, which is typically found in the restrained joint.⁽¹⁵⁾ This is also evident by the plots of the residual stresses transverse to the welding direction alongside the top of the joints assigned to Figure 12.

With increasing distance from the weld centreline the transverse residual stresses first slightly increase then establish a sharp tensile peak of about 920 MPa and 700 MPa for the first joint and about 900 and 1000 MPa for the second joint in the restraint length of $L_2 = 55$ mm near the fusion line and gradually decrease to a minimum value of about 230 MPa.

As the restraint length gets longer ($L_2 = 110$ mm), the transverse tensile stresses become smaller as shown in Figure 12. Not only have the stress levels been changed, but the sharp tensile peak seems also to be more balanced. This can be noticed from the sharp tensile peak at about 870 MPa and 800 MPa for the first joint and about 900 and 940 MPa for the second joint. Again, such stress levels gradually decrease to a minimum value of about 115 MPa.

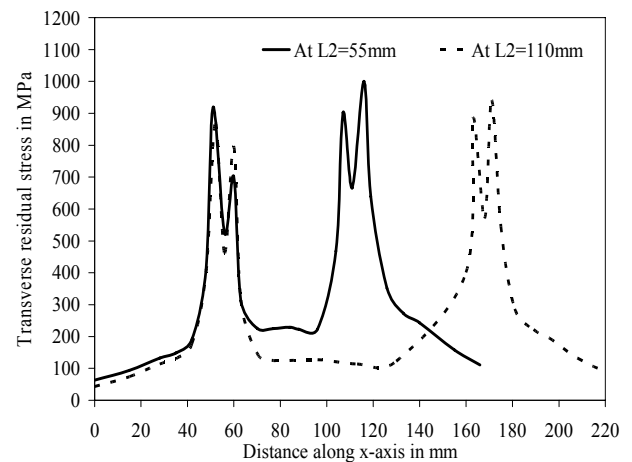


Figure 12. Residual stresses transverse to the welding direction at the top of the joints after cooling down to room temperature at rigid restraint

Some remarks may be considered for the above results:

1. The residual stresses showed inhomogeneous contours. This is due to the fact that heat from the first joint (deposited in between L_1 and L_2) dissipates to an area of the second joint (deposited in between L_2 and L_3), but it only influences one

side of base material. Therefore, the residual stress contours are inhomogeneous.

2. As represented in Figure 10 and Figure 11, the maximum residual stresses have been identified in the weld metal area, in particular adjacent to the fusion line. Additionally, such stresses are significantly changed with panel length (restraint length No. 2, L2). For instance, at the panel length of $L2 = 55$ mm the maximum stress of 1348 MPa occurs beneath the top surface of the second joint (right hand side) at the fusion line, while the wider panel (at the restraint length of $L2 = 110$ mm) decreases the maximum residual stress level to 1232 MPa. These findings show that a critical spot for failure risk is located on the top side near the fusion line of the last joint. These results also show a good agreement with the previous contributions^(3, 15) in that a typically maximum residual stress is located beside the last welded pass.

3. In general, the highest residual stress can reach the yield strength level of the base material.^(2, 16) In these results, the S 1100QL represents a yield strength and ultimate tensile strength of about 1150 MPa and 1348 MPa, respectively. This means that in a real welding situation the rigid restraint must be avoided for many seams because the rigid restraint condition significantly introduces plastic deformation in the welded component for this material.

4. As described in the introduction, the total restraint level can be calculated and changed by combining three factors, i.e. weld edge preparation, plate dimension and an external force. In these three-welded plates, such total restraint level is varied by changing panel length (L2). For the present study, it also shows the same trend as shown in a previous contribution.⁽³⁾ It demonstrated that the decrease of the residual stress with increasing restraint length (L2) to the weld centreline is smaller. At butt joint, furthermore the restraint level increases with plate thickness and with decreasing restraint length (L2). It may be concluded from these results that plate dimension has to be carefully designed in order to reduce the residual stress level.

5. Another important point is used to explain why residual stresses are different when various restraint lengths have been performed. Considering that the thermal heat conduction is significantly changing with the plate dimension, this effect can be attributed to the differences in the

temperature distribution and therefore to the various influences of phase transformation on the residual stresses of various restraint lengths.

Welding Residual Stresses in Single V-Butt Joints of Two and Three-Welded Plates

Figure 13 shows the residual stress contours transverse to the welding direction in two-welded plates after cooling down to room temperature for a rigidly clamped S 1100 QL root joint. Normally, the root is located asymmetrically to the neutral axis of the joint and thus, the stresses increase from compression at the root to tension at the top of the weld. The highest tensile stresses of about 1129 MPa are thus located near the top surface at the fusion line (Figure 13).

Again, residual-stresses at the specific nodes along x-axis beneath the top surface are selected to be plotted as shown in Figure 14. At the top surface of the joint the values show the typical M-shape curve.

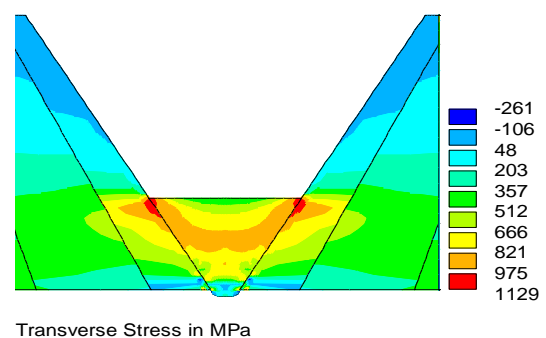


Figure 13. FEM calculated residual stresses distribution transverse to the welding direction in two-welded plates for a rigidly clamped S1100 QL root joint

As shown by comparison of Figure 12 and Figure 14, the residual-stress distribution in two-welded plates is more symmetrical than that in three-welded plates. Beside the maximum residual stress in the three-welded plates is higher than in the two-welded plates. This is connected with the fact that the first joint (in three-welded plates) has been welded completely before the last joint is being welded. Therefore, the first joint inhibits movement of the last joint during welding and cooling. It may be said that each weld seems to be a stiffener of the other when there are many seams deposited side by side.

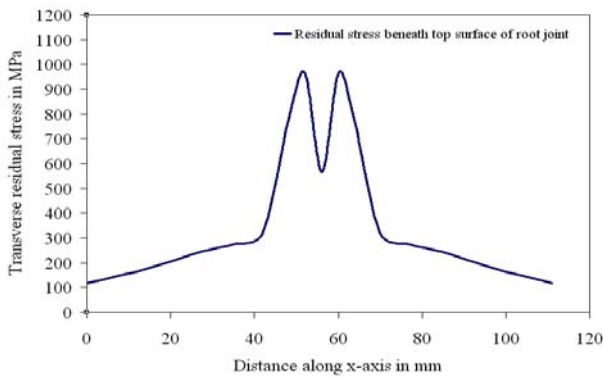


Figure 14. Transverse residual stresses distribution along x-axis in two-welded plates for a rigidly clamped S 1100 QL root joint

Conclusions

From the first investigations of the welding residual stresses in two competing single V-butt joints, the following conclusions can be drawn:

1. The highest residual stress level in three-welded plates of single V-butt joints has been identified in the weld metal adjacent to the fusion line which is the same as in welding of two-welded plates. In contrast to the previously investigated symmetric two plate joint, the residual stress distribution is not homogeneous, in particular because the welds were carried out and were cooled after each other. In other words, this is a result from the welding sequence as shown in Figure 6b.

2. In order to avoid higher residual stress in more than two-welded plates, and to reduce restraint intensity from plate dimension view point (RFy2) the restraint length (L2) should be applied in a distance of more than 110 mm from a weld.. However, this effect has to be further studied in order to clarify an appropriate restraint length for the real welding construction.

3. As elucidated by the numerical simulation, the residual stresses in three-welded plates can achieve under the same conditions, a much higher level than those in two-welded plates. This has to be attributed to the fact that the first welded plate cannot move freely. Also, an additional temperature field is produced with the second weld contributing to an additional respective straining and stress build-up in the joint. This is particular the case for the last weld seam, showing the highest stresses. In

future, the effects of the time passing between completion of the first joint and starting the next weld on the stress build-up will be investigated.

Perspectives

The present study is only the beginning of welding procedures for cold cracking avoidance in three-welded plates of S 1100 QL. Further studies should put the following points into focus.

1. In the real situation of welding construction, it is usual to apply a multi-pass welding process. Although, many studies reported on weld cracks in multi-pass welds, it is very difficult to locate information concerning detailed mechanical behaviour of multi-pass joints in the entire course of welding. Therefore, a further study has to evaluate, in particular, effects of welding sequences on stress distribution in multi-pass welds of three-welded plates with the same material, dimension and external force as applied in this study.

2. Another important point is preparing restraint length (L2) and residual stress level diagram providing data to assess the failure risk of welded construction from the view point of welding design.

3. As shown in previous papers,⁽¹⁷⁾ it is frequently anticipated that a controlled interpass temperature in addition to, and without, preheating might reduce the residual stresses in multi-layer welds. With respect to practical applications, such assumptions have also to be reconsidered regarding the shrinkage restraint. Without restraint, a controlled interpass temperature and preheating might reduce the residual stresses after cooling to room-temperature in high strength structural steel butt joints. However, the opposite might be the case if such multi-layer joints are welded at rigidity restraint corresponding to real welded components. It is still a challenging task to evaluate welding procedure in terms of controlled interpass temperature and preheating in multi-pass welds, in particular for three-welded plates.

4. Hydrogen is a major factor for HACC in welded component. Therefore, hydrogen diffusion analysis and hydrogen removal heat treatment procedure have been clarified by using FEM.

5. Finally, all of the above targets should be evaluated together in order to determine cold cracking behavior in three-welded plates.

Acknowledgement

The author would like to acknowledge Prof. Dr.-Ing. Thomas Böellinghaus, (Vice President of the Federal Institute for Materials Research and Testing, Berlin) for the fruitful discussions.

References

- Hipp, K.J. and Hoffmeister, H. 1980, Zur Prüfung von Schweißverbindungen im instrumentierten Einspannversuch (in German). Prüfverfahren zur Beurteilung der Kaltrissanfälligkeit von Stählen, DVS-Bericht 64, DVS, Düsseldorf : 35-39.
- Gordon, R. 1997. Welding, brazing and soldering : Joint evaluation and quality control. In : *ASM Welding Handbook*. Vol. 6: 1073-1124.
- Böellinghaus, Th., Kannengießer, Th. and Neuhaus, M. *Effects of the structural restraint intensity on the stress-strain build up in butt joint Mathematical Modelling of Weld Phenomena 7*. H. Cerjak edition. London : IOM, : 651-669.
- Kannengießer, Th., Böellinghaus, Th., Florian, W. and Herold, H. 2001. Effect of weld metal strength and welding conditions on reaction forces and stress distribution of restraint component. *Welding in the World*. **45(1/2)** : 18-26.
- Wahab, M.A., Alam, M.S., Painter M.J. and Stafford, P.E. 2006. Experimental and numerical simulation of restraining forces in gas metal arc welded joints. *Welding J. (February)* : 35-43s.
- Satoh, K., Ueda, Y., Kihara H. et al. 1973. Recent trends of research into restraint stresses and strains in relation to weld cracking. *Welding in the World*. **11(5/6)** : 133-156.
- Satoh, K., Ueda, Y., Kihara H. et al. Recent trends of researches on restraint stresses and strains in weld cracking. IIW doc. IX-788-72.
- Wongpanya, P., Böellinghaus, Th. and Lothongkum, G. 2006. Effects of hydrogen removal heat treatment on residual stresses in high strength structural steel welds. *Welding in the World*. **50** : 96-103.
- Hoffmeister, H. 1986. Concept and procedure description of the IRC test for assessing hydrogen assisted weld cracking. *Comp. Steel Research*. **57(7)** : 73-78. and IIW doc. IX-1369-85.
- Richter, F. 1973. *Die Wichtigsten Physikalischen Eigenschaften von 52 Eisenwerkstoffen*. Heft 8, Verlag Stahleisen, Düsseldorf.
- Zimmer, P., Seeger D.M. and Böellinghaus, Th. Hydrogen permeation and related material properties of high strength structural steels. In: *Proceedings of High Strength Steels for Hydropower Plants*. Graz, 5-6 July 2005, no. 17.
- Zimmer, P., Böellinghaus, Th. and Kannengießer, Th. *Effects of hydrogen on weld microstructure and mechanical properties of high strength structural steels S690Q and S1100QL*. IIW doc. II-A-141-04.
- Goldak, J. A. and Akhlaghi, M. 2005. *Computational welding mechanics*. Springer : Science & Business Media : 321.
- Böellinghaus, Th. and Hoffmeister, H. *Finite element calculations of pre- and postheating procedures for sufficient hydrogen removal in butt joints. Mathematical Modelling of Weld Phenomena 3*, H. Cerjak edition, London : IOM : 276-756.
- Leung, C.K., Pick, R.J. and Mok, D.H.B. 1990. Finite element modeling of a single pass weld. *Welding Res. Council Bull.* **356 (August)** : 42.
- Bailey, N. 1994. *Weldability of ferritic steels*. *ASM International*. Cambridge : Abington Publishing : 286.
- Wongpanya, P., Böellinghaus, Th. and Lothongkum, G. 2008. Way to reduce the cold cracking risk in high strength structural steel welds. *International Conference of the International Institute of Welding*, 25-29 May. Johannesburg, South Africa.